Durham University

On the use of the Material Point Method for large rotation problems

Lei Wang, **Will Coombs**, Charles Augarde & Michael Cortis

Associate Professor in Computational Mechanics

Department of Engineering, Durham University, UK

w.m.coombs@durham.ac.uk

www.screwpilesforoffshorewind.co.uk

14th June 2018

(implicit) Material Point Method focus at Durham University

seabed ploughing (Cortis)

screwpile installation (Wang)

overcoming volumetric locking (CMAME, 2018)

IGA-based MPM (Ghaffari-Motlagh)

B-spline representation & enforcement of boundaries (Bing)

generalised interpolation & gradient plasticity (Charlton)

(implicit) Material Point Method focus at Durham University

seabed ploughing (Cortis)

screwpile installation (Wang)

overcoming volumetric locking (CMAME, 2018)

IGA-based MPM (Ghaffari-Motlagh)

B-spline representation & enforcement of boundaries (Bing)

generalised interpolation & gradient plasticity (Charlton)

Background

Screwpiles for wind energy foundation systems

- Designing foundations for offshore wind turbines is challenging because of the complex dynamic mechanical loading environment;
- monopiles are currently the most commonly used foundation in the offshore wind market due to their ease of installation;
- this research is part of a larger UK research council funded grant investigating alternative foundation solutions for offshore wind.

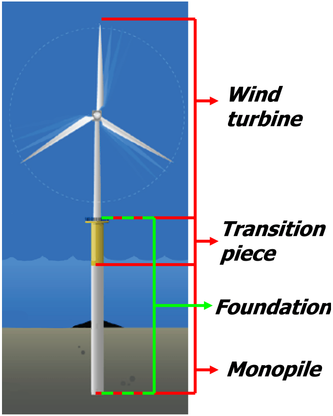

Background

Screwpiles for wind energy foundation systems

- Designing foundations for offshore wind turbines is challenging because of the complex dynamic mechanical loading environment;
- monopiles are currently the most commonly used foundation in the offshore wind market due to their ease of installation;
- this research is part of a larger UK research council funded grant investigating alternative foundation solutions for offshore wind.

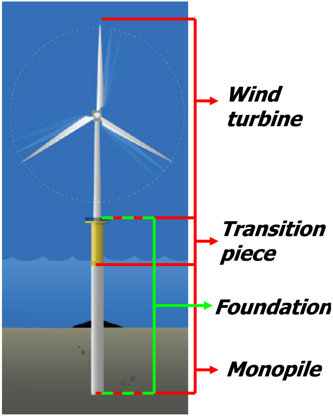

Background

Screwpiles for wind energy foundation systems

- The research aims to make screw piles a more attractive foundation (or anchoring) option for offshore wind farms;
- installation torque in different seabed conditions is a key question;
- computational modelling of screw pile installation is Durham's focus;
- challenging problem: truly 3D, large deformation, non-linear material behaviour - MPM appears to be ideal?

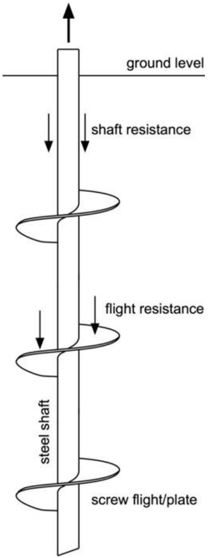

Background

Screwpiles for wind energy foundation systems

- The research aims to make screw piles a more attractive foundation (or anchoring) option for offshore wind farms;
- installation torque in different seabed conditions is a key question;
- computational modelling of screw pile installation is Durham's focus;
- challenging problem: truly 3D, large deformation, non-linear material behaviour - MPM appears to be ideal?

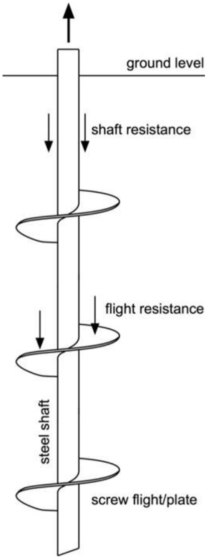

Implicit material point formulation

governing equations

governing equation of elasticity

$$\nabla \sigma_{ij} + {f_i}^b = 0 \quad \text{in} \quad \Omega$$

subject to the following

$$u_i = g_i \quad \text{on} \quad \partial\Omega_D \qquad \text{and} \qquad \sigma_{ij} n_j = t_i \quad \text{on} \quad \partial\Omega_N$$

where g_i and t_i are the Dirichlet and Neumann boundary conditions

discretised into the conventional updated Lagrangian form

$$\int_{\varphi_t(E)} [\nabla S_{vp}]^T \{\sigma\} \mathrm{d}v - \int_{\varphi_t(E)} [S_{vp}]^T \{b\} \mathrm{d}v - \int_{\varphi_t(\partial\Omega_N)} [S_{vp}]^T \{t\} \mathrm{d}s = \{0\}$$

Implicit material point formulation

governing equations

governing equation of elasticity

$$\nabla \sigma_{ij} + {f_i}^b = 0 \quad \text{in} \quad \Omega$$

subject to the following

$$u_i = g_i \quad \text{on} \quad \partial\Omega_D \qquad \text{and} \qquad \sigma_{ij} n_j = t_i \quad \text{on} \quad \partial\Omega_N$$

where g_i and t_i are the Dirichlet and Neumann boundary conditions

discretised into the conventional updated Lagrangian form

$$\int_{\varphi_t(E)} [\nabla S_{vp}]^T \{\sigma\} \mathrm{d}v - \int_{\varphi_t(E)} [S_{vp}]^T \{b\} \mathrm{d}v - \int_{\varphi_t(\partial\Omega_N)} [S_{vp}]^T \{t\} \mathrm{d}s = \{0\}$$

Implicit material point formulation

finite deformation mechanics

linear isotropic relationship is assumed between elastic logarithmic strains and Kirchhoff stresses

$$\tau_{ij} = D^{\mathsf{e}}_{ijkl}\varepsilon^{\mathsf{e}}_{kl} \qquad \text{where} \qquad \varepsilon^{\mathsf{e}}_{ij} = \frac{1}{2}\ln\left(F^{\mathsf{e}}_{ik}F^{\mathsf{e}}_{jk}\right)$$

and the deformation gradient is obtained as

$$F_{ij} = \frac{\partial x_i}{\partial X_j} \qquad \text{and} \qquad F_{ij} = F^{\mathsf{e}}_{ik}F^{\mathsf{p}}_{kj}$$

the Cauchy stress is recovered using

$$\sigma_{ij} = \frac{1}{J}\tau_{ij} \qquad \text{where} \qquad J = \det\left(F_{ij}\right)$$

the adopted stress and strain measures provide the most straightforward way of implementing large strain elasto-plasticity

Implicit material point formulation

finite deformation mechanics

linear isotropic relationship is assumed between elastic logarithmic strains and Kirchhoff stresses

$$\tau_{ij} = D^{\mathsf{e}}_{ijkl}\varepsilon^{\mathsf{e}}_{kl} \qquad \text{where} \qquad \varepsilon^{\mathsf{e}}_{ij} = \frac{1}{2}\ln\left(F^{\mathsf{e}}_{ik}F^{\mathsf{e}}_{jk}\right)$$

and the deformation gradient is obtained as

$$F_{ij} = \frac{\partial x_i}{\partial X_j} \qquad \text{and} \qquad F_{ij} = F^{\mathsf{e}}_{ik}F^{\mathsf{p}}_{kj}$$

the Cauchy stress is recovered using

$$\sigma_{ij} = \frac{1}{J}\tau_{ij} \qquad \text{where} \qquad J = \det\left(F_{ij}\right)$$

the adopted stress and strain measures provide the most straightforward way of implementing large strain elasto-plasticity

Implicit material point formulation

finite deformation mechanics

linear isotropic relationship is assumed between elastic logarithmic strains and Kirchhoff stresses

$$\tau_{ij} = D^{\mathsf{e}}_{ijkl}\varepsilon^{\mathsf{e}}_{kl} \qquad \text{where} \qquad \varepsilon^{\mathsf{e}}_{ij} = \frac{1}{2}\ln\left(F^{\mathsf{e}}_{ik}F^{\mathsf{e}}_{jk}\right)$$

and the deformation gradient is obtained as

$$F_{ij} = \frac{\partial x_i}{\partial X_j} \qquad \text{and} \qquad F_{ij} = F^{\mathsf{e}}_{ik}F^{\mathsf{p}}_{kj}$$

the Cauchy stress is recovered using

$$\sigma_{ij} = \frac{1}{J}\tau_{ij} \qquad \text{where} \qquad J = \det\left(F_{ij}\right)$$

the adopted stress and strain measures provide the most straightforward way of implementing large strain elasto-plasticity

Implicit material point formulation

finite deformation mechanics

linear isotropic relationship is assumed between elastic logarithmic strains and Kirchhoff stresses

$$\tau_{ij} = D^{\mathsf{e}}_{ijkl}\varepsilon^{\mathsf{e}}_{kl} \qquad \text{where} \qquad \varepsilon^{\mathsf{e}}_{ij} = \frac{1}{2}\ln\left(F^{\mathsf{e}}_{ik}F^{\mathsf{e}}_{jk}\right)$$

and the deformation gradient is obtained as

$$F_{ij} = \frac{\partial x_i}{\partial X_j} \qquad \text{and} \qquad F_{ij} = F^{\mathsf{e}}_{ik}F^{\mathsf{p}}_{kj}$$

the Cauchy stress is recovered using

$$\sigma_{ij} = \frac{1}{J}\tau_{ij} \qquad \text{where} \qquad J = \det\left(F_{ij}\right)$$

the adopted stress and strain measures provide the most straightforward way of implementing large strain elasto-plasticity

Implicit material point formulation

finite deformation mechanics: deformation gradient update

A point of departure of implicit MP methods from conventional finite elements is the calculation of the deformation gradient

$$F_{ij} = \Delta F_{ik} F^n_{kj} \qquad \text{where} \qquad \Delta F_{ij} = \delta_{ij} + \frac{\partial \Delta u_i}{\partial \tilde{X}_j}$$

and $\tilde{X}_i = x_i - \Delta u_i$ are the coordinates at the start of the loadstep.

However, equilibrium is satisfied in the updated frame, requiring mapping of the shape function derivatives

$$\frac{\partial S_{vp}}{\partial x_i} = \frac{\partial S_{vp}}{\partial \tilde{X}_j}\frac{\partial \tilde{X}_j}{\partial x_i} = \frac{\partial S_{vp}}{\partial \tilde{X}_j}(\Delta F_{ji})^{-1}$$

Note that the spatial derivatives are needed to integrate the stiffness and internal force contribution of a material point in an updated Lagrangian formulation.

Implicit material point formulation

finite deformation mechanics: deformation gradient update

A point of departure of implicit MP methods from conventional finite elements is the calculation of the deformation gradient

$$F_{ij} = \Delta F_{ik} F^n_{kj} \qquad \text{where} \qquad \Delta F_{ij} = \delta_{ij} + \frac{\partial \Delta u_i}{\partial \tilde{X}_j}$$

and $\tilde{X}_i = x_i - \Delta u_i$ are the coordinates at the start of the loadstep.

However, equilibrium is satisfied in the updated frame, requiring mapping of the shape function derivatives

$$\frac{\partial S_{vp}}{\partial x_i} = \frac{\partial S_{vp}}{\partial \tilde{X}_j}\frac{\partial \tilde{X}_j}{\partial x_i} = \frac{\partial S_{vp}}{\partial \tilde{X}_j}(\Delta F_{ji})^{-1}$$

Note that the spatial derivatives are needed to integrate the stiffness and internal force contribution of a material point in an updated Lagrangian formulation.

Implicit material point formulation

finite deformation mechanics: deformation gradient update

A point of departure of implicit MP methods from conventional finite elements is the calculation of the deformation gradient

$$F_{ij} = \Delta F_{ik} F^n_{kj} \qquad \text{where} \qquad \Delta F_{ij} = \delta_{ij} + \frac{\partial \Delta u_i}{\partial \tilde{X}_j}$$

and $\tilde{X}_i = x_i - \Delta u_i$ are the coordinates at the start of the loadstep.

However, equilibrium is satisfied in the updated frame, requiring mapping of the shape function derivatives

$$\frac{\partial S_{vp}}{\partial x_i} = \frac{\partial S_{vp}}{\partial \tilde{X}_j}\frac{\partial \tilde{X}_j}{\partial x_i} = \frac{\partial S_{vp}}{\partial \tilde{X}_j}(\Delta F_{ji})^{-1}$$

Note that the spatial derivatives are needed to integrate the stiffness and internal force contribution of a material point in an updated Lagrangian formulation.

Numerics & implicit implementation

basis functions

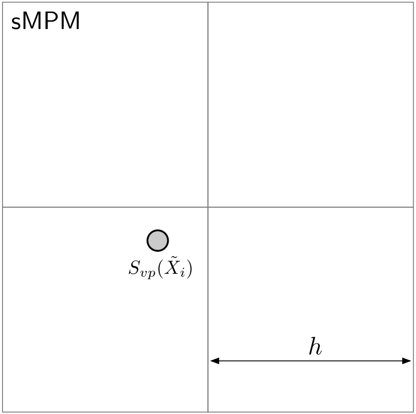

$$
\begin{aligned}
S_{vp} &= 1 + (\tilde{X}_p - \tilde{X}_v)/h & -h &< \tilde{X}_p - \tilde{X}_v \leq 0 \\
S_{vp} &= 1 - (\tilde{X}_p - \tilde{X}_v)/h & 0 &< \tilde{X}_p - \tilde{X}_v \leq h,
\end{aligned}
$$

Numerics & implicit implementation

basis functions

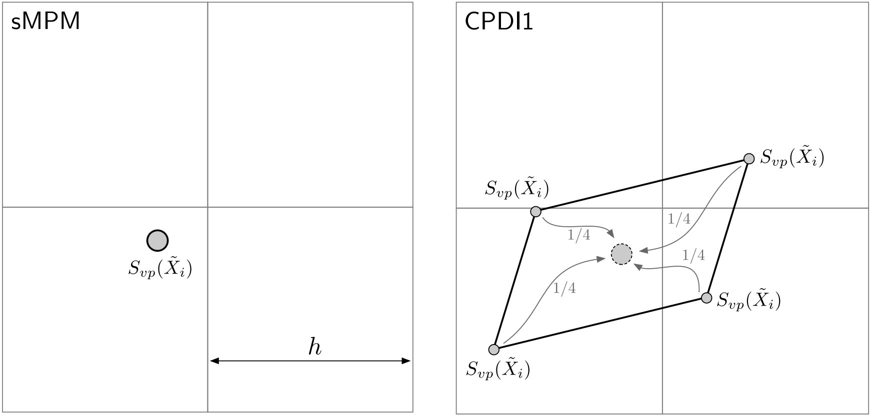

$$S_{vp} = 1 + (\tilde{X}_p - \tilde{X}_v)/h \qquad -h < \tilde{X}_p - \tilde{X}_v \leq 0$$
$$S_{vp} = 1 - (\tilde{X}_p - \tilde{X}_v)/h \qquad 0 < \tilde{X}_p - \tilde{X}_v \leq h,$$

Numerics & implicit implementation

basis functions

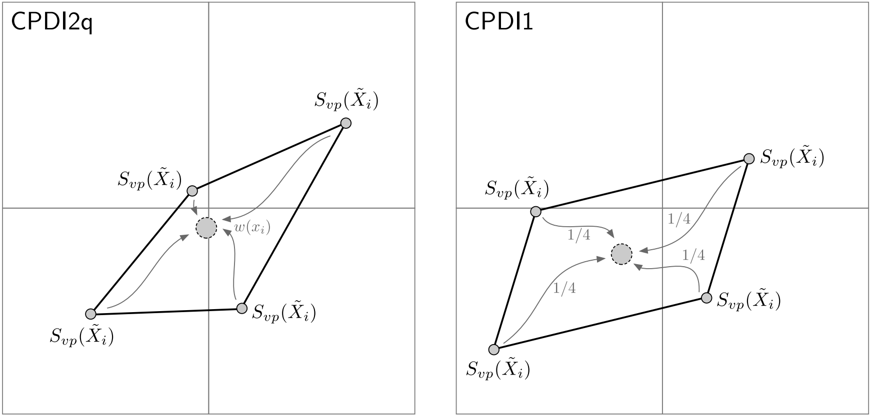

$$
\begin{aligned}
S_{vp} &= 1 + (\tilde{X}_p - \tilde{X}_v)/h & \quad -h &< \tilde{X}_p - \tilde{X}_v \leq 0 \\
S_{vp} &= 1 - (\tilde{X}_p - \tilde{X}_v)/h & \quad 0 &< \tilde{X}_p - \tilde{X}_v \leq h,
\end{aligned}
$$

Numerics & implicit implementation

basis functions

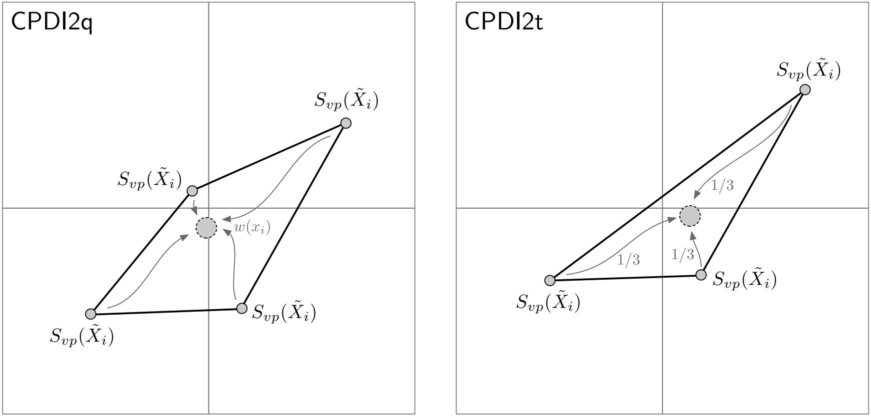

$$S_{vp} = 1 + (\tilde{X}_p - \tilde{X}_v)/h \qquad -h < \tilde{X}_p - \tilde{X}_v \leq 0$$
$$S_{vp} = 1 - (\tilde{X}_p - \tilde{X}_v)/h \qquad 0 < \tilde{X}_p - \tilde{X}_v \leq h,$$

Numerics & implicit implementation

non-linear solution

fully implicit Newton process used to solve the non-linear equation

$$\{f^{oobf}\} = \{f^{int}\} + \{f^{ext}\} = \{0\}$$

where

$$\{f^{int}\} = \mathop{\mathrm{A}}_{\forall p} \left(\left[\nabla S_{vp}\right]^T \{\sigma_p\} V_p \right) \quad \text{and}$$

$$\{f^{ext}\} = \int_{\varphi_t(\partial\Omega_N)} [S_{vp}]^T \{t\} ds + \mathop{\mathrm{A}}_{\forall p} \left([S_{vp}]^T \{f^b\} V_p \right)$$

global consistent tangent determined analytically for optimal convergence

(linearisation of the internal force with respect to the unknown displacements)

Numerics & implicit implementation

non-linear solution

fully implicit Newton process used to solve the non-linear equation

$$\{f^{oobf}\} = \{f^{int}\} + \{f^{ext}\} = \{0\}$$

where

$$\{f^{int}\} = \mathop{\mathsf{A}}_{\forall p} \left(\left[\nabla S_{vp}\right]^T \{\sigma_p\} V_p \right) \quad \text{and}$$

$$\{f^{ext}\} = \int_{\varphi_t(\partial\Omega_N)} [S_{vp}]^T \{t\} ds + \mathop{\mathsf{A}}_{\forall p} \left([S_{vp}]^T \{f^b\} V_p \right)$$

global consistent tangent determined analytically for optimal convergence

(linearisation of the internal force with respect to the unknown displacements)

Numerics & implicit implementation

computational procedure

For each loadstep:

1. assemble the internal force stiffness contribution of all material points;
2. increment the external tractions and/or body forces in and solve for the nodal displacements within a loadstep using the Newton process;
3. update material point positions, stresses, volumes, domains, etc.;
4. reset or replace the background grid.

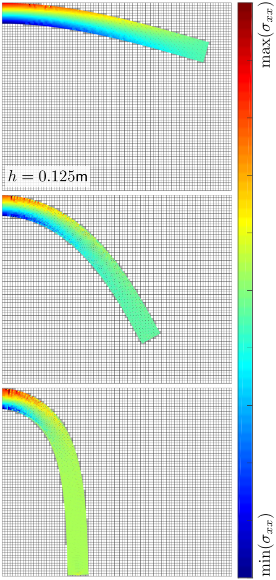

Numerics & implicit implementation

computational procedure

For each loadstep:

1. assemble the internal force stiffness contribution of all material points;
2. increment the external tractions and/or body forces in and solve for the nodal displacements within a loadstep using the Newton process;
3. update material point positions, stresses, volumes, domains, etc.;
4. reset or replace the background grid.

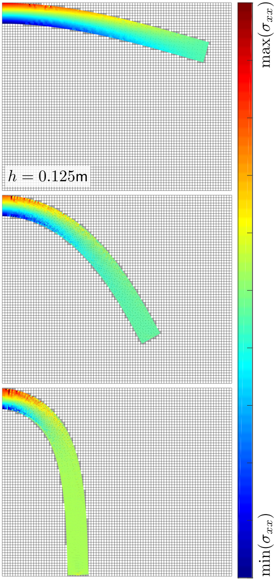

Numerics & implicit implementation

computational procedure

For each loadstep:

1. assemble the internal force stiffness contribution of all material points;
2. increment the external tractions and/or body forces in and solve for the nodal displacements within a loadstep using the Newton process;
3. update material point positions, stresses, volumes, domains, etc.;
4. reset or replace the background grid.

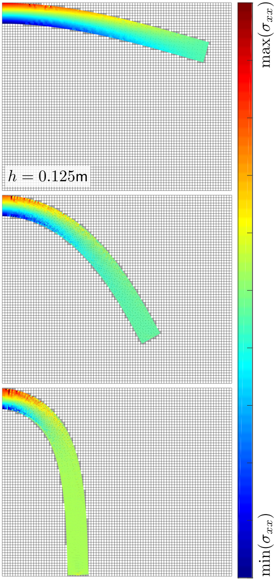

Numerical examples
simple stretch (validation)

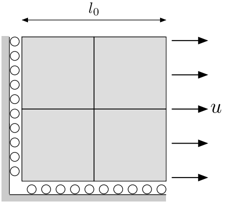

- $l_0 = 2$, $h = 1$
- $E = 10^3$, $\nu = 0$
- von Mises, $\rho_y = 400$
- 2^2 MPs/element
- plane strain
- moving mesh, edge displacement $u/l_0 = 2$

Numerical examples

simple stretch (validation)

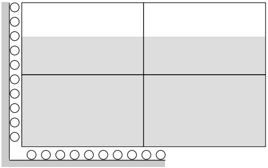

- $l_0 = 2$, $h = 1$
- $E = 10^3$, $\nu = 0$
- von Mises, $\rho_y = 400$
- 2^2 MPs/element
- plane strain
- moving mesh, edge displacement $u/l_0 = 2$

Numerical examples

simple stretch (validation)

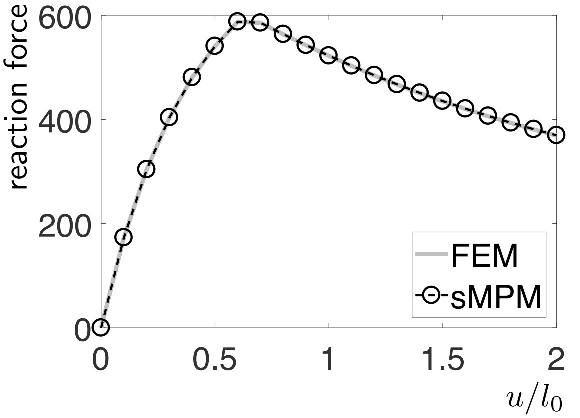

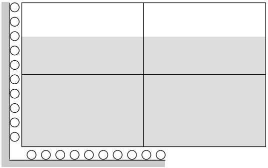

- $l_0 = 2,\ h = 1$
- $E = 10^3,\ \nu = 0$
- von Mises, $\rho_y = 400$
- 2^2 MPs/element
- plane strain
- moving mesh, edge displacement $u/l_0 = 2$

Numerical examples

simple stretch (validation)

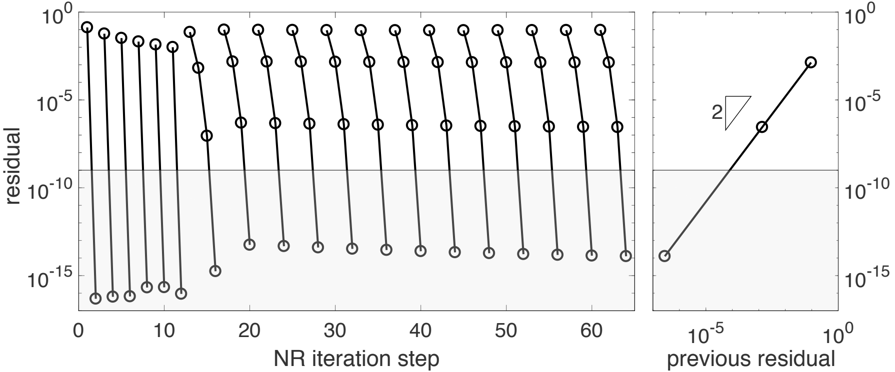

Numerical examples

corner stretch

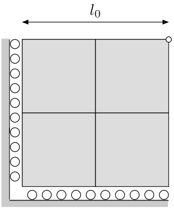

- $l_0 = 2$, $h = 1$
- $E = 10^3$, $\nu = 0.4$
- elastic behaviour
- 2^2 & 8^2 MPs/e
- plane strain
- moving mesh, corner displacement $\Delta x, \Delta y = 4$

Numerical examples

corner stretch

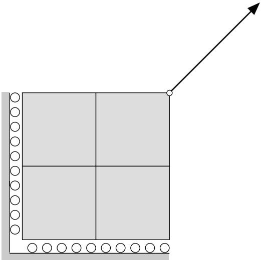

- $l_0 = 2$, $h = 1$
- $E = 10^3$, $\nu = 0.4$
- elastic behaviour
- 2^2 & 8^2 MPs/e
- plane strain
- moving mesh, corner displacement $\Delta x, \Delta y = 4$

Numerical examples

corner stretch

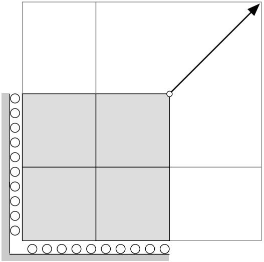

- $l_0 = 2,\ h = 1$
- $E = 10^3,\ \nu = 0.4$
- elastic behaviour
- 2^2 & 8^2 MPs/e
- plane strain
- moving mesh, corner displacement $\Delta x, \Delta y = 4$

Numerical examples

corner stretch

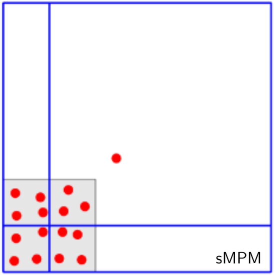

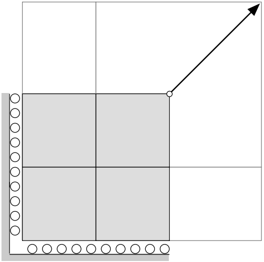

- $l_0 = 2,\ h = 1$
- $E = 10^3,\ \nu = 0.4$
- elastic behaviour
- 2^2 & 8^2 MPs/e
- plane strain
- moving mesh, corner displacement $\Delta x, \Delta y = 4$

Numerical examples

corner stretch

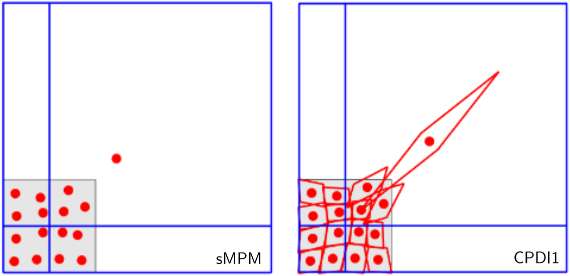

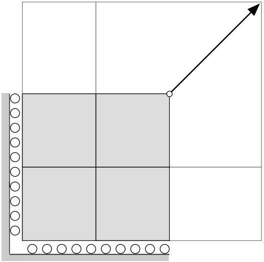

- $l_0 = 2,\ h = 1$
- $E = 10^3,\ \nu = 0.4$
- elastic behaviour
- 2^2 & 8^2 MPs/e
- plane strain
- moving mesh, corner displacement $\Delta x, \Delta y = 4$

Numerical examples

corner stretch

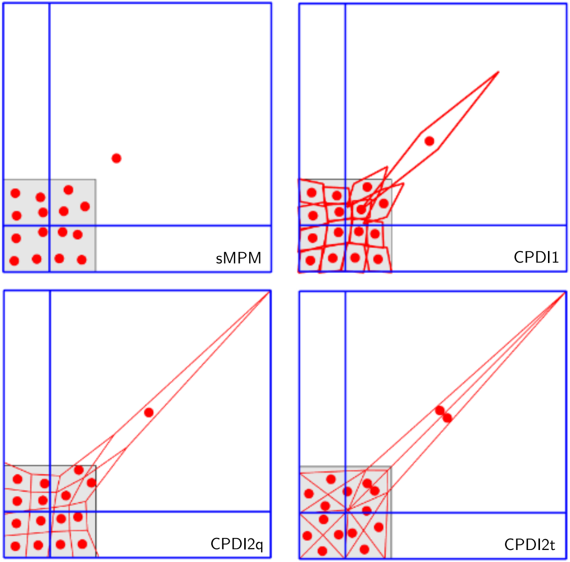

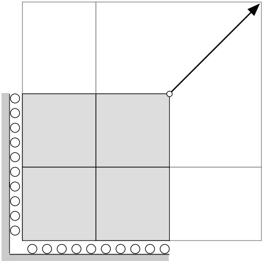

- $l_0 = 2,\ h = 1$
- $E = 10^3,\ \nu = 0.4$
- elastic behaviour
- 2^2 & 8^2 MPs/e
- plane strain
- moving mesh, corner displacement $\Delta x, \Delta y = 4$

Numerical examples

corner stretch

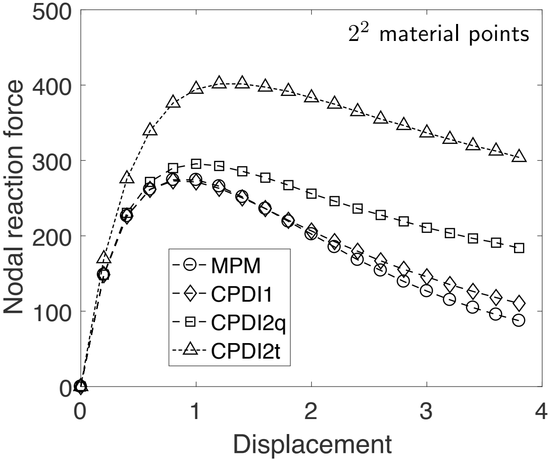

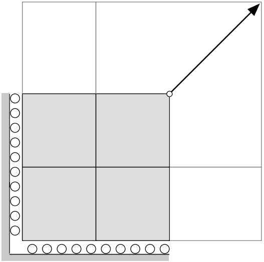

- $l_0 = 2,\ h = 1$
- $E = 10^3,\ \nu = 0.4$
- elastic behaviour
- 2^2 & 8^2 MPs/e
- plane strain
- moving mesh, corner displacement $\Delta x, \Delta y = 4$

Numerical examples

corner stretch

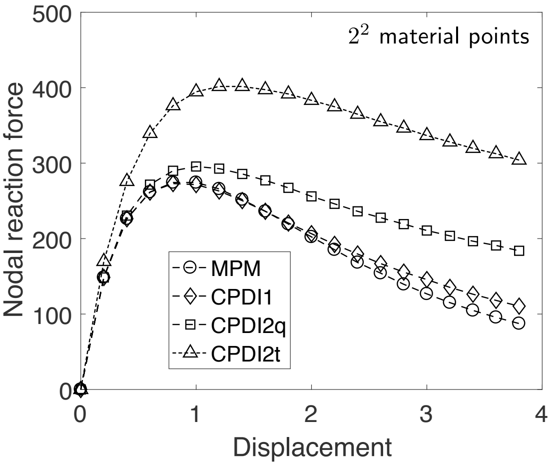

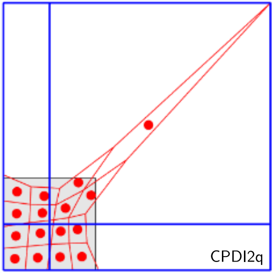

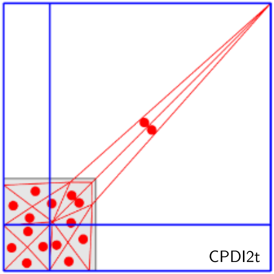

Numerical examples

corner stretch

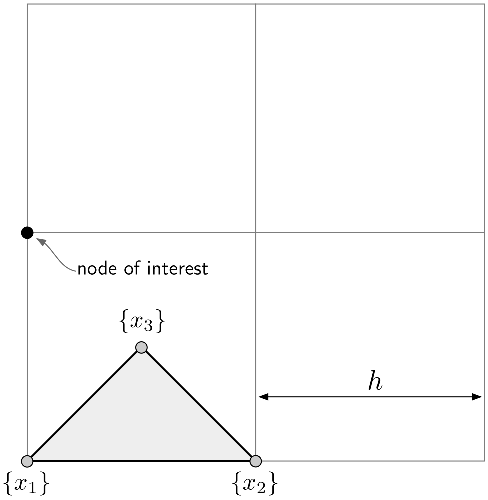

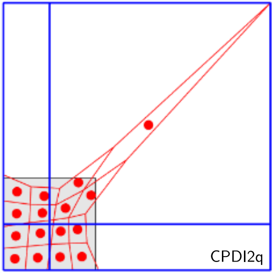

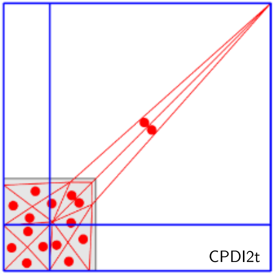

Numerical examples

corner stretch

$$\nabla S_{vp} = \frac{1}{2V_p}\left(S_v(\{x_1\})\begin{Bmatrix} y_2 - y_3 \\ x_3 - x_2 \end{Bmatrix} + S_v(\{x_2\})\begin{Bmatrix} y_3 - y_1 \\ x_1 - x_3 \end{Bmatrix} + S_v(\{x_3\})\begin{Bmatrix} y_1 - y_2 \\ x_2 - x_1 \end{Bmatrix}\right)$$

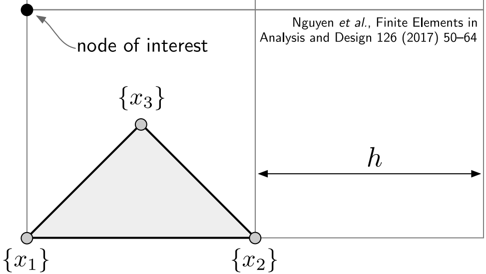

Nguyen *et al.*, Finite Elements in Analysis and Design 126 (2017) 50–64

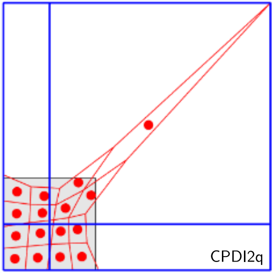

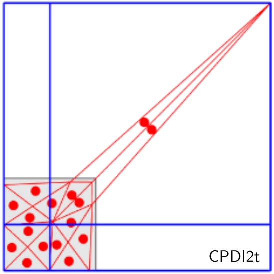

Numerical examples

corner stretch

$$\nabla S_{vp} = \frac{1}{2V_p}\left(\cancelto{0}{S_v(\{x_1\})} \begin{Bmatrix} y_2 - y_3 \\ x_3 - x_2 \end{Bmatrix} + \cancelto{0}{S_v(\{x_2\})} \begin{Bmatrix} y_3 - y_1 \\ x_1 - x_3 \end{Bmatrix} + \cancelto{1/4}{S_v(\{x_3\})} \begin{Bmatrix} y_1 - y_2 \\ x_2 - x_1 \end{Bmatrix} \right)$$

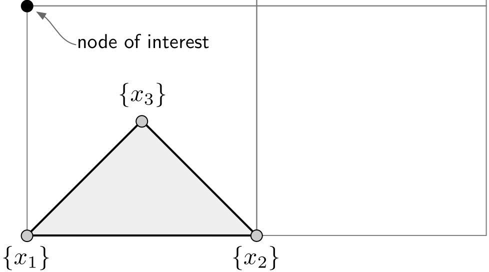

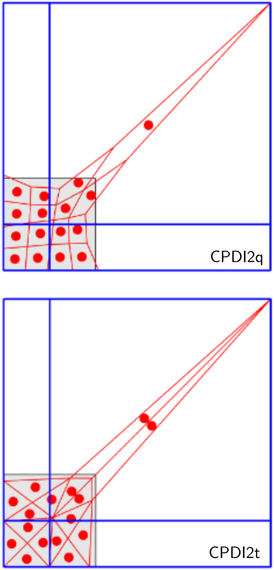

Numerical examples

corner stretch

$$\nabla S_{vp} = \frac{1}{2V_p}\left(S_v(\{x_1\}) \begin{Bmatrix} y_2 - y_3 \\ x_3 - x_2 \end{Bmatrix} + S_v(\{x_2\}) \begin{Bmatrix} y_3 - y_1 \\ x_1 - x_3 \end{Bmatrix} + S_v(\{x_3\}) \begin{Bmatrix} y_1 - y_2 \\ x_2 - x_1 \end{Bmatrix} \right)$$

$$\nabla S_{vp} = \frac{1}{2V_p}\left(1/4 \begin{Bmatrix} 0 \\ h \end{Bmatrix} \right)$$

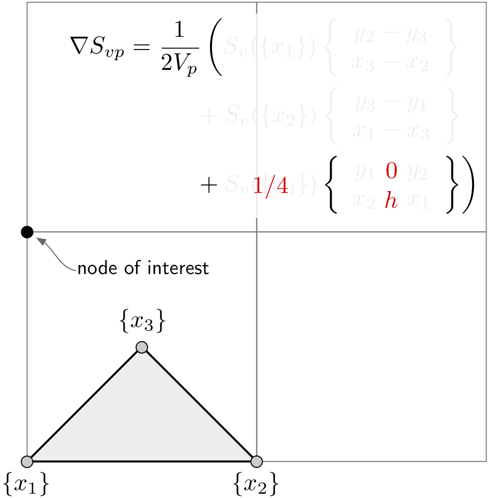

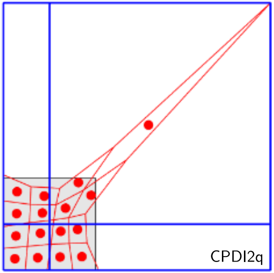

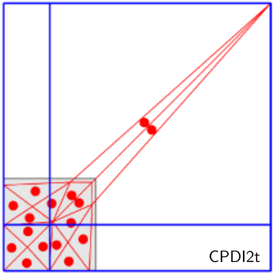

Numerical examples

corner stretch

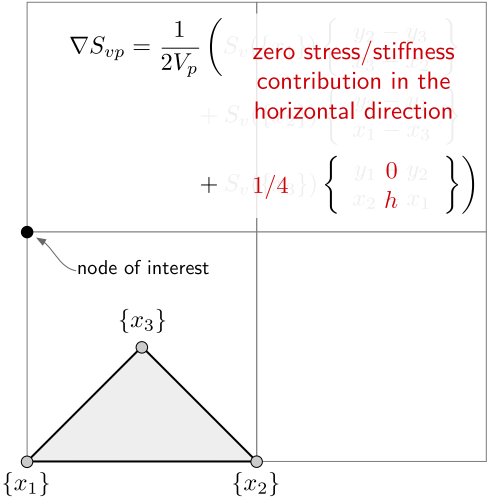

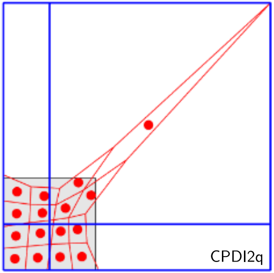

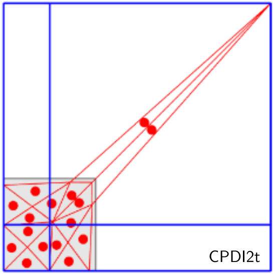

Numerical examples

corner stretch

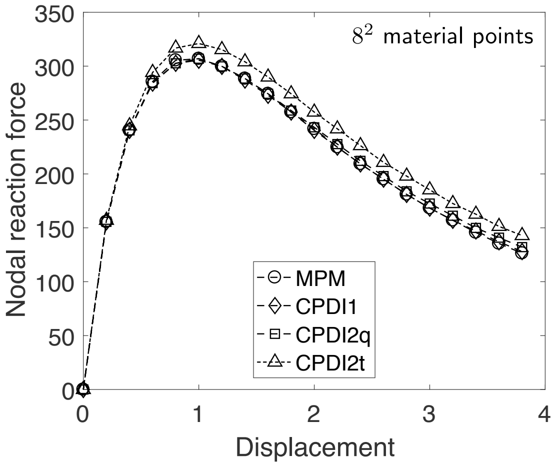

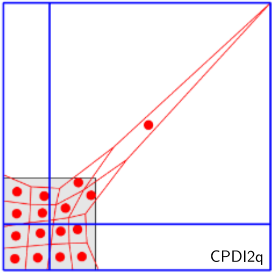

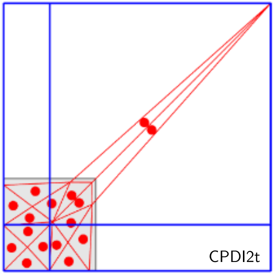

Numerical examples

doughnut twist

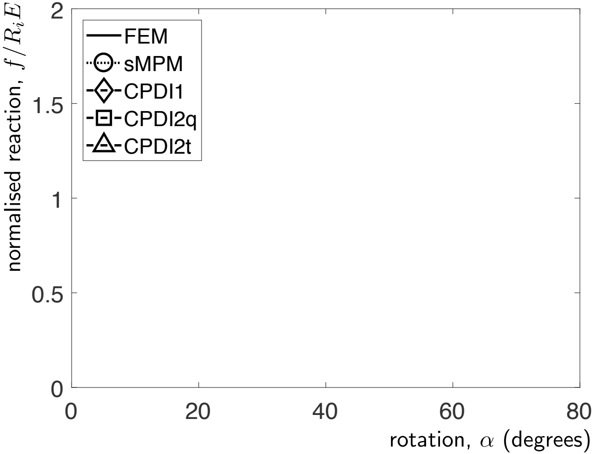

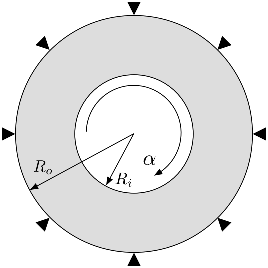

- $R_o = 10,\ R_i = 5$
- $E = 10^6,\ \nu = 0$
- von Mises, $\rho_y = 10^6$
- 2^2 MPs/element
- plane strain

fixed outer boundary and incremental rotation $\Delta\alpha$ on inner boundary with rotational moving mesh

Numerical examples

doughnut twist

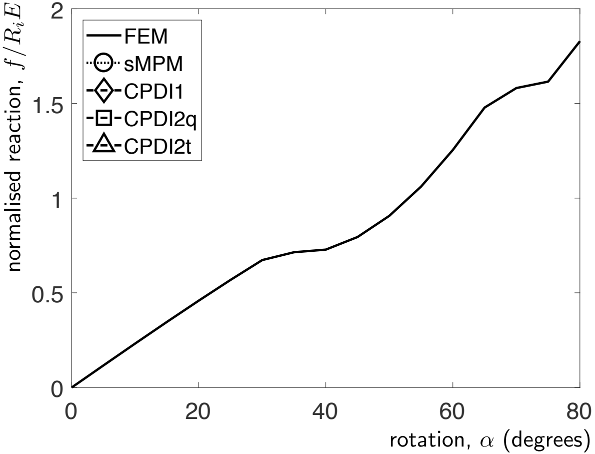

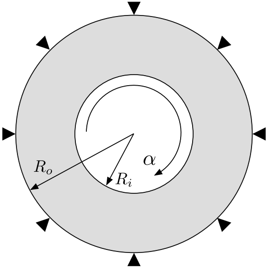

- $R_o = 10, \; R_i = 5$
- $E = 10^6, \; \nu = 0$
- von Mises, $\rho_y = 10^6$
- 2^2 MPs/element
- plane strain

fixed outer boundary and incremental rotation $\Delta\alpha$ on inner boundary with rotational moving mesh

Numerical examples

doughnut twist

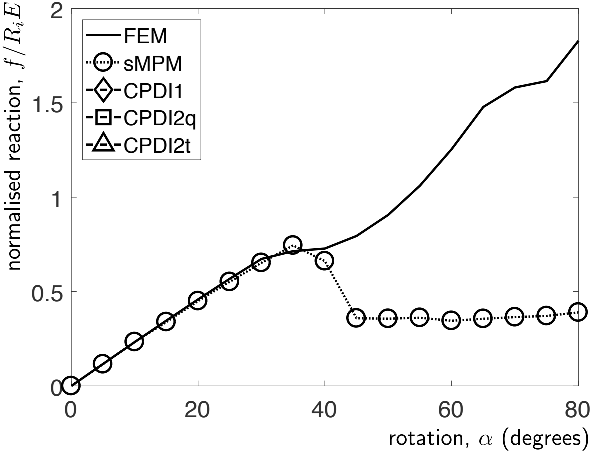

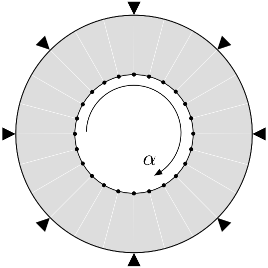

- $R_o = 10, \ R_i = 5$
- $E = 10^6, \ \nu = 0$
- von Mises, $\rho_y = 10^6$
- 2^2 MPs/element
- plane strain

fixed outer boundary and incremental rotation $\Delta\alpha$ on inner boundary with rotational moving mesh

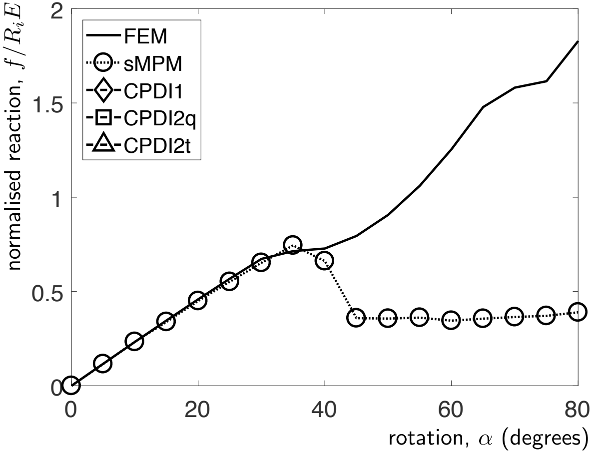

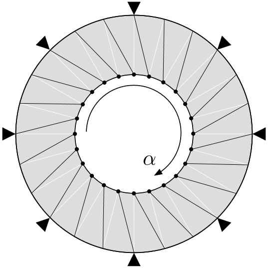

- $R_o = 10,\ R_i = 5$
- $E = 10^6,\ \nu = 0$
- von Mises, $\rho_y = 10^6$
- 2^2 MPs/element
- plane strain

fixed outer boundary and incremental rotation $\Delta\alpha$ on inner boundary with rotational moving mesh

Numerical examples

doughnut twist

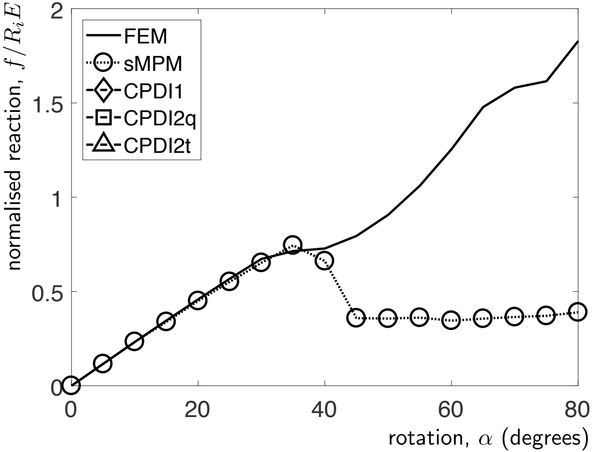

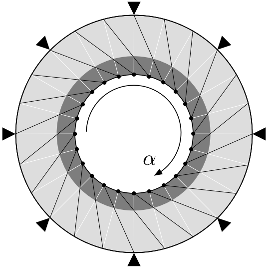

- $R_o = 10$, $R_i = 5$
- $E = 10^6$, $\nu = 0$
- von Mises, $\rho_y = 10^6$
- 2^2 MPs/element
- plane strain

fixed outer boundary and incremental rotation $\Delta\alpha$ on inner boundary with rotational moving mesh

Numerical examples

doughnut twist

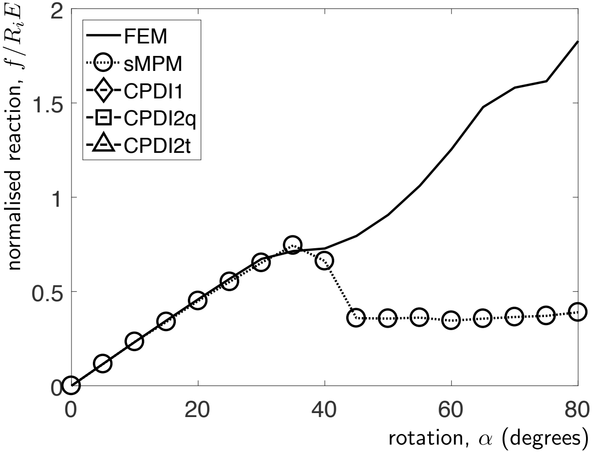

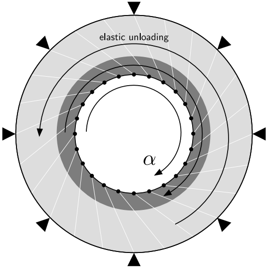

- $R_o = 10,\ R_i = 5$
- $E = 10^6,\ \nu = 0$
- von Mises, $\rho_y = 10^6$
- 2^2 MPs/element
- plane strain

fixed outer boundary and incremental rotation $\Delta\alpha$ on inner boundary with rotational moving mesh

Numerical examples

doughnut twist

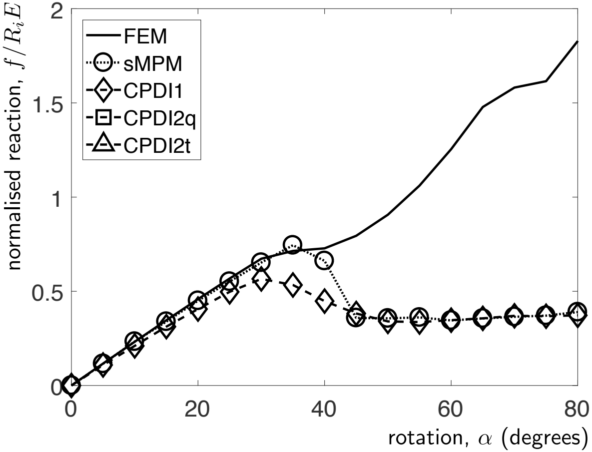

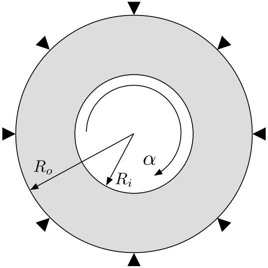

- $R_o = 10$, $R_i = 5$
- $E = 10^6$, $\nu = 0$
- von Mises, $\rho_y = 10^6$
- 2^2 MPs/element
- plane strain

fixed outer boundary and incremental rotation $\Delta\alpha$ on inner boundary with rotational moving mesh

Numerical examples

doughnut twist

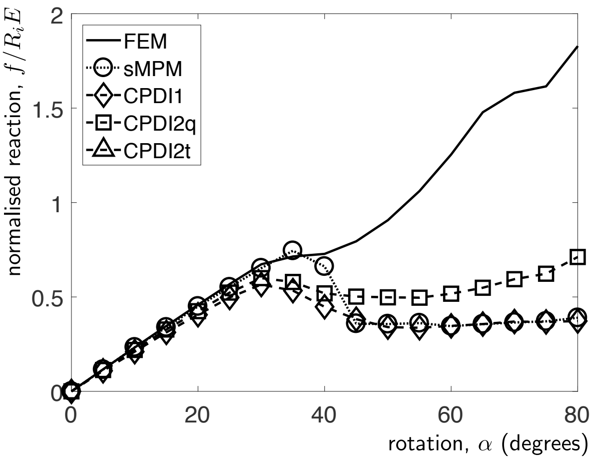

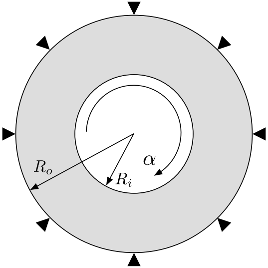

- $R_o = 10$, $R_i = 5$
- $E = 10^6$, $\nu = 0$
- von Mises, $\rho_y = 10^6$
- 2^2 MPs/element
- plane strain

fixed outer boundary and incremental rotation $\Delta\alpha$ on inner boundary with rotational moving mesh

Numerical examples

doughnut twist

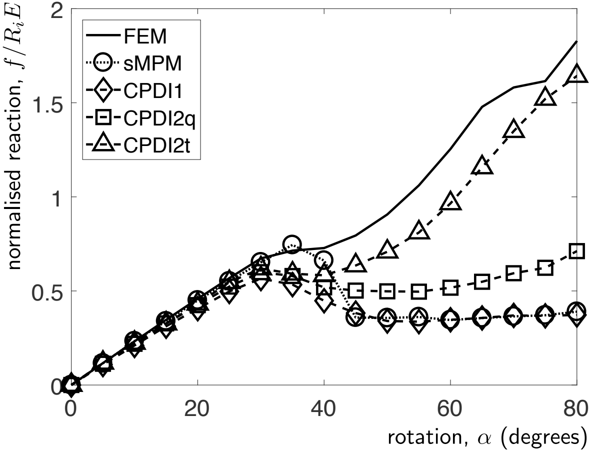

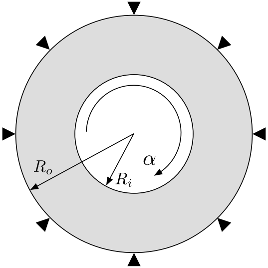

- $R_o = 10$, $R_i = 5$
- $E = 10^6$, $\nu = 0$
- von Mises, $\rho_y = 10^6$
- 2^2 MPs/element
- plane strain

fixed outer boundary and incremental rotation $\Delta\alpha$ on inner boundary with rotational moving mesh

Numerical examples

doughnut twist

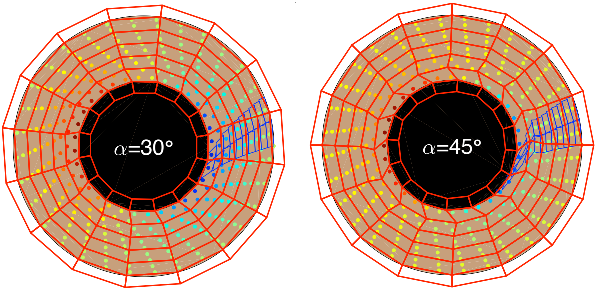

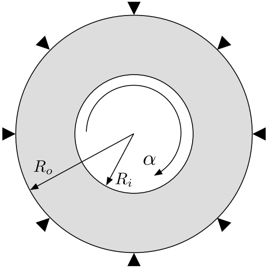

- $R_o = 10,\ R_i = 5$
- $E = 10^6,\ \nu = 0$
- von Mises, $\rho_y = 10^6$
- 2^2 MPs/element
- plane strain

fixed outer boundary and incremental rotation $\Delta\alpha$ on inner boundary with rotational moving mesh

Numerical examples

doughnut twist

Durham University

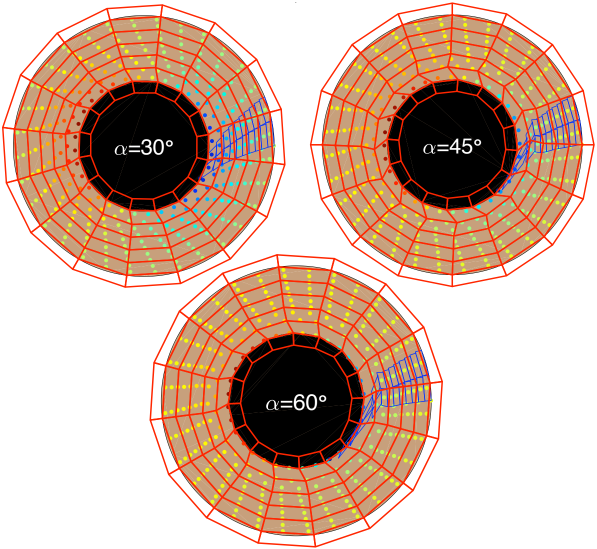

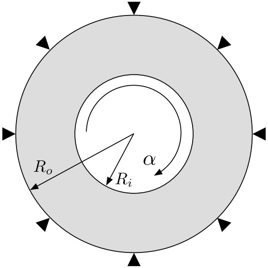

- $R_o = 10$, $R_i = 5$
- $E = 10^6$, $\nu = 0$
- von Mises, $\rho_y = 10^6$
- 2^2 MPs/element
- plane strain

fixed outer boundary and incremental rotation $\Delta\alpha$ on inner boundary with rotational moving mesh

Observations

- A unified implicit computational framework for sMPM and CPDIs has been developed;
- moving mesh concept extended to include rotational deformation;
- CPDI approaches reduce the instabilities inherent in material point methods; but
- only the sMPM and CPDI1 approaches obtain physically meaningful solutions for large rotational problems;
- CPDI2q faces issues due to distortion of particle domains; and
- CPDI2t has degenerative cases with spurious spatial derivatives of the basis functions.

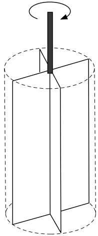

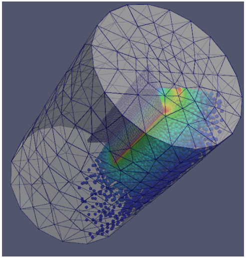

Observations

- A unified implicit computational framework for sMPM and CPDIs has been developed;
- moving mesh concept extended to include rotational deformation;
- CPDI approaches reduce the instabilities inherent in material point methods; but
- only the sMPM and CPDI1 approaches obtain physically meaningful solutions for large rotational problems;
- CPDI2q faces issues due to distortion of particle domains; and
- CPDI2t has degenerative cases with spurious spatial derivatives of the basis functions.

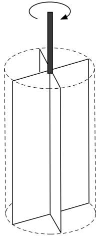

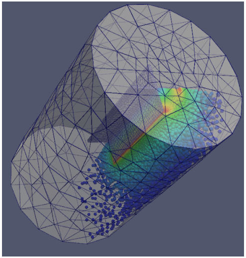

Acknowledgements

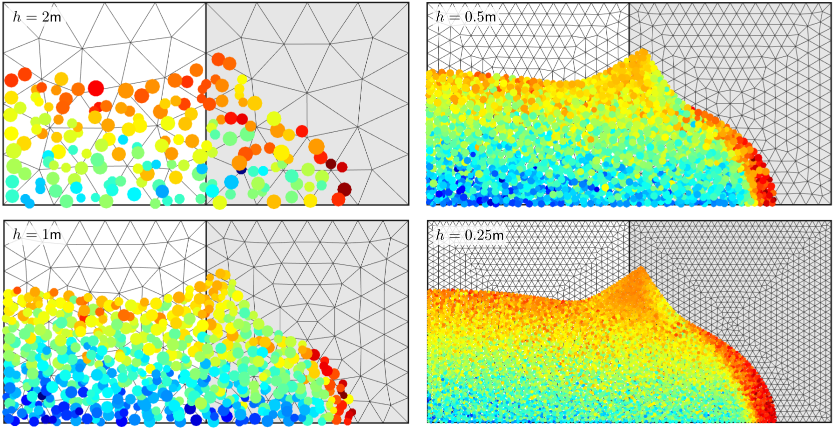

The research presented is the work of Dr Lei Wang supported by the Engineering and Physical Sciences Research Council (EPSRC) grant EP/N006054/1: *Screw piles for wind energy foundation systems*.

On the use of the Material Point Method for large rotation problems

Lei Wang, **Will Coombs**, Charles Augarde & Michael Cortis

Associate Professor in Computational Mechanics

Department of Engineering, Durham University, UK

w.m.coombs@durham.ac.uk

www.screwpilesforoffshorewind.co.uk

14th June 2018